H1.6.

Theoretical and empirical studies of metapopulations: population and genetic dynamics of the *Silene–Ustilago* system

Peter H. Thrall and Janis Antonovics

Abstract: Host–pathogen population dynamics may often only be understood by a multifaceted approach designed to understand processes at a regional as well as local scale. We have investigated the regional population dynamics of the anther-smut *Ustilago violacea*, a pollinator-transmitted fungal disease, and its plant host *Silene alba*, using descriptive, experimental, and theoretical approaches. A 7-year survey of multiple natural populations revealed persistence of host and pathogen despite a high rate of population turnover. In an experimental metapopulation, disease spread was greater and more rapid in populations that were relatively isolated or had a previous history of disease occurrence. A computer simulation showed that spatial substructuring can drastically alter expectations based on analytical results from single population models of host–pathogen systems. Moreover, the simulation reproduced many of the patterns detected in the long-term survey and predicted that healthy populations should be more resistant than diseased ones, as found experimentally.

Key words: metapopulations, host–pathogen dynamics, spatial models, anther-smut diseases.

Résumé : La dynamique des populations hôte–pathogènes peut souvent n'être comprise que par une approche à facettes multiples, conçue pour comprendre les processus à l'échelle régionale aussi bien que locale. Les auteurs ont examiné la dynamique des populations régionales du charbon de l'anthère, *Ustilago violacea*, une maladie fongique transmise par les pollinisateurs, et sa plante hôte, le *Silene alba*, en utilisant les approches descriptives expérimentales et théoriques. Un suivi pendant 7 ans de nombreuses populations naturelles révèle la persistence de l'hôte et du pathogène, en dépit d'un taux de cyclage élevé des populations. Dans une métapopulation expérimentale, la dispersion de la maladie est plus importante et plus rapide dans les populations qui sont relativement isolées ou ont une histoire préalable d'incidence de la maladie. Une simulation sur ordinateur montre que la sous-structure spatiale peut perturber fortement les attentes basées sur les résultats analitiques de modèles basés sur une seule population de systèmes hôte–pathogène. De plus, la simulation reproduit plusieurs des patrons décelés dans le suivi à long terme et prédit que les populations saines devraient être plus résistantes que celles qui sont malades, tels que montré expérimentalement.

Mots clés : métapopulation, dynamique hôte–pathogène, modèle spatial, maladie du charbon des anthères.
[Traduit par la rédaction]

The *Silene–Ustilago* host–pathogen system

Silene alba is a short-lived dioecious perennial found along roadsides and in other ruderal habitats, having spread throughout eastern North America since its introduction from Europe in the mid-1800s (McNeill 1977). The anther-smut *Ustilago violacea* is present in both European and North American populations of *S. alba*, but it is unknown how or when the pathogen became established in North America. Neither a recent plant fungal index (Farr et al. 1989) nor several earlier ones (Clinton 1904; Seymour 1929) record *Ustilago violacea* on *S.* (=*Lychnis*) *alba*, even though it is recorded on several other species in the Caryophyllaceae. Farlow and Seymour (1888) record *U. violacea* on an undetermined *Lychnis* sp. However, Baker (1947) states that the disease in North America is "rare (if not completely absent)."

The biology of the *Silene–Ustilago* interaction has been detailed previously (e.g., Baker 1947; Alexander and Antonovics 1988; Alexander 1990*a*; Thrall et al. 1993*b*); we therefore give only a brief outline here. In dioecious species such as *S. alba*, *U. violacea* causes male flowers to produce teliospore-filled anthers but no pollen, and it causes female flowers to undergo a sex switch so they also produce spore-filled anthers, with the ovary developing only as a sterile rudimentary structure. The teliospores are transmitted to new hosts by insect pollinators (Baker 1947; Hassan and MacDonald 1971; Lee 1981; Jennersten 1983, 1988; Alexander and Antonovics 1988; Thrall et al. 1993*b*) and newly diseased flowers appear within 3 weeks to 2 months (Alexander 1990*b*) after the fungus has grown into the host and entered newly developing flower buds (Batcho and Audran 1980). By the following year, the plant usually becomes systemically infected

Received August 15, 1994.

P.H. Thrall[1] and J. Antonovics. Department of Botany, Duke University, Durham, NC 27708, U.S.A.

[1] Author to whom all correspondence should be addressed.

and all the flowers are diseased, resulting in complete sterility. Seed-borne transmission is absent (Baker 1947; but see Brefeld 1921), but passive transmission can occur if spores fall onto seedlings close to diseased plants (Alexander and Maltby 1991).

Anther-smut diseases are pollinator transmitted and so can be regarded as examples of plant venereal diseases (Alexander and Antonovics 1988; Thrall et al. 1993*a*). Furthermore, the disease caused by *U. violacea* has a number of features in common with animal sexually transmitted diseases (STDs), including localized sites of infection, causing sterility in the host, and having a moderate or negligible effect on host survival (Holmes 1983; Felman 1986; Alexander and Antonovics 1988; Thrall et al. 1993*a*; Lockhart, Thrall, and Antonovics, unpublished data).

In this paper we illustrate the importance of an integrative approach involving field observations, experiments, and computer simulation in assessing the influence of variation in population spacing and genetic resistance on disease dynamics and the coexistence of host and pathogen. We show further how these different approaches interact synergistically to provide not only a novel view of host–pathogen systems, but also new insights into more general ecological and evolutionary processes in spatially subdivided populations (i.e., metapopulations).

Factors affecting population dynamics of sexually transmitted diseases (STDs): general considerations

It has become clear in recent years that the stability of host–parasite and predator–prey assemblages is strongly influenced by spatial substructuring (Levins 1969; Caswell 1978; Hanski and Gilpin 1991). We have shown that explicit metapopulation structures (Antonovics 1994) or more simple interconnected sets of populations spanning a uniform habitat can result in coexistence in STD systems that would otherwise not persist in a single patch (J. Antonovics, M.P. Hassell and H.N. Comins, unpublished data). Such coexistence is characterized by a wide range of spatial and temporal dynamics, including regions of spiral waves and spatial chaos (cf. Hassell et al. 1991; Comins et al. 1992). Spatial structure also has important repercussions for host–pathogen coevolution (Frank 1993), and for stability of genetic polymorphisms in general. Host–pathogen dynamics are characterized by interactions that can be strongly density and frequency dependent (Levin and Udovic 1977) and it has long been argued (Gilpin 1975) that spatial or group substructuring can greatly affect evolutionary outcomes in such situations. More recently it has been shown that less efficient/virulent parasitoids can invade a spatially structured population (Boerlijst et al. 1993) whereas such invasion is impossible in an unstructured population. From a purely ecological perspective, May and Anderson (1990) have shown that if human immunodeficiency virus (HIV) has persisted in human populations for over a century (as suggested by levels of sequence divergence between simian and human lentiviruses), then this persistence is readily explainable by spatial models allowing for sexual contacts within and among rural villages; changes in intervillage migration could explain the recent spread of the disease. Clearly, evolutionary and ecological analyses need to incorporate the spatial effects that are almost universal in real ecological situations.

In STDs such as the *Silene–Ustilago* system, the probability of a healthy individual becoming infected will be more dependent on the frequency of infectives (Getz and Pickering 1983; Antonovics et al. 1994*a*; Thrall et al. 1993*a*, 1994) in the population than on the density of infectives, as is usually modelled for airborne and other indirectly transmitted diseases (e.g., Anderson and May 1981). Frequency-dependent transmission arises in systems where the number of host individuals contacted by a disease vector or the number of sexual contacts between individuals remains constant over a range of population densities. In such cases, disease transmission will be primarily determined by the probability that a contacted individual is infective. Frequency-dependent transmission will be distinct from density-dependent transmission whenever population size varies; because diseases in natural systems are likely to affect population size, the study of STDs requires a modelling formulation in which rates of disease transmission depend on frequency (Antonovics 1994).

Theoretical studies on the local population dynamics of systems with frequency-dependent disease transmission have shown that coexistence is difficult to achieve without some form of disease-independent host regulation (Getz and Pickering 1983; Antonovics 1992; Thrall et al. 1993*a*, 1994). However, certain features can broaden conditions for coexistence in STD systems relative to ordinary infectious diseases; these conditions are broadest when density-dependent regulation acts more strongly on the healthy class (e.g., through effects on juveniles), the disease causes sterility rather than added mortality, and there is no host recovery (Thrall et al. 1993*a*, 1994).

The issue of coexistence is complicated by the likelihood that host–pathogen systems are genetically variable. To assess whether genetic composition is likely to affect population dynamics (and vice versa), we have explicitly investigated the conditions for polymorphism in host resistance and susceptibility, simultaneously incorporating genetic and numerical dynamics in models of single populations. Such polymorphisms broaden the region for coexistence (Antonovics 1992, 1994) and polymorphism in disease resistance is more likely when the difference in resistance conferred by alternate alleles is large rather than small (Antonovics and Thrall 1994). Indeed, when allelic differences in resistance are large, polymorphism is possible over a wide range of costs of resistance, including situations where costs are minimal (Antonovics and Thrall 1994).

Studies of disease spread in experimental field populations of *S. alba*, where transmission rates were manipulated using genetic variation in host resistance, have confirmed the applicability of models with frequency-dependent transmission (Thrall and Jarosz 1994*a*, 1994*b*). These studies also showed that genetic composition had large effects on the qualitative nature of the dynamics. Moreover, these empirical and modelling studies indicated that the most likely outcome in nature would not be the disease driving host populations to extinction, but the loss of the pathogen (Thrall and Jarosz 1994*b*), suggesting that host–pathogen coexistence may indeed be difficult to achieve in nature. Nevertheless, results from long-term censuses of natural populations of *S. alba* and *U. violacea* (see below) indicate that not only can disease levels be quite high (as much as 80%) but also the disease can persist over extended periods of time. Surveys of natural populations of

Table 1. Data taken from the roadside census of the natural metapopulation during the years 1988–1993.

Year	No. of populations	Population size: healthy	Population size: diseased	% occupied sites with disease	Frequency of disease
1988	259	14.55(2.64)	26.60(5.40)	20.59(11.68)	0.34(0.06)
1989	412	14.07(3.14)	44.30(8.59)	15.71(11.82)	0.24(0.05)
1990	428	10.47(2.82)	25.44(4.71)	17.72(12.47)	0.28(0.04)
1991	494	9.66(2.19)	22.61(4.01)	18.62(13.18)	0.25(0.03)
1992	460	16.71(4.85)	27.61(8.29)	16.25(10.71)	0.30(0.04)
1993	435	13.97(4.74)	15.86(2.88)	16.34(13.41)	0.42(0.09)

NOTE: Values shown are means across all sites occupied for at least 1 year. Frequency of disease is the mean frequency of disease only considering populations that had disease present (values in parentheses are standard errors).

Table 2. Host and pathogen colonization and extinction rates calculated from the census of roadside populations.

	1988–1989	1989–1990	1990–1991	1991–1992	1992–1993
Host					
Colonization rate	0.56	0.20	0.29	0.15	0.17
Extinction rate	0.12	0.20	0.14	0.21	0.22
Pathogen					
Colonization rate	0.69	0.45	0.25	0.25	0.23
Extinction rate	0.19	0.27	0.23	0.36	0.29

NOTE: Rates are calculated as the number of new/extinct populations per existing healthy or diseased population per year.

S. alba and *U. violacea* have also indicated that local populations have high extinction and colonization rates (Antonovics et al. 1994*b*) and this population turnover may be an important additional factor in the dynamics of this system.

Field observations: the roadside census

Since 1988 we have conducted surveys of *S. alba* and *U. violacea* along 150 km of roadside (treating both sides independently) within an approximately 25 × 25 km area of Giles county, Virginia (see Antonovics et al. 1994*b*). Within this area, we defined populations as the number of healthy and infected individuals in a 40-m segment of roadside or psilon. Our definition of what constitutes a population was based on reasons of practicality as well as biology. First, it is generally difficult to delineate population boundaries in nature except in some situations (e.g., island systems). Second, 40-m segments can easily be relocated using a car odometer. Finally, both seed and spore dispersal are limited such that the scale of 40 m encompasses at least one, but not many, fungal and host genetic neighborhoods (Alexander 1990*b*; Antonovics et al. 1994*b*). When we analyzed the census data, pooling adjacent psilons by groups of two or four, there was no effect on overall patterns of disease incidence (e.g., relationship between population size and percent infection).

During the first 2 weeks of June of each year, roadsides were censused for the number of healthy male and female plants, and the number of infected plants. A total of 7500 segments were included; between 400 and 500 were occupied at any one time and 70 or so of these had disease present (Table 1). The census results for the first 6 years indicated a high rate of population turnover, with substantial colonization and extinction for both host and the pathogen (Table 2). Colonization and extinction processes were dependent both on population size and proximity to other populations (Antonovics et al. 1994*b*).

Experimental studies: an artificial metapopulation

To explore the consequences of population connectedness on disease spread, in 1992 we established replicate sets of experimental populations along a 3-km section of fence line within a large open cattle pasture in the vicinity of Mountain Lake Biological station (MLBS), Virginia (Fig. 1). Each replicate consisted of six populations spaced at graded intervals chosen to encompass values greater and less than the 40-m segments used in the roadside census (5, 10, 20, 40, and 80 m); replicates were separated by a minimum of 160 m to minimize the likelihood of spore movement between them. Each population consisted of 24 healthy and one diseased plant planted in a 5 × 5 m array of 20-cm pots at 1-m intervals. This spacing was chosen because it is a representative density in nature and large enough to reduce stochastic effects on disease spread (e.g., due to nonoverlap in phenology of infected and healthy individuals). Within each population, the diseased plant was placed in the central position, and the healthy plants were assigned randomly to the remaining positions. All populations were enclosed by electric fencing to exclude deer and cattle.

To test the hypothesis that resistance structure might be related to population history (for example, diseased populations might have higher levels of resistance than populations that had never been exposed to the pathogen), healthy plants

Fig. 1. Map of the experimental metapopulation (located at latitude 37°22′20″ N and longitude 80°30′ W; not to scale). Replicates are numbered 1–6 on the map; double solid lines are paved roads, double dashed lines are gravel drives, and dotted solid lines are fences. The lower portion of the figure shows the spatial distribution of populations within each replicate; each filled square represents a single population (each population contains 24 healthy and 1 diseased (inoculated) plant).

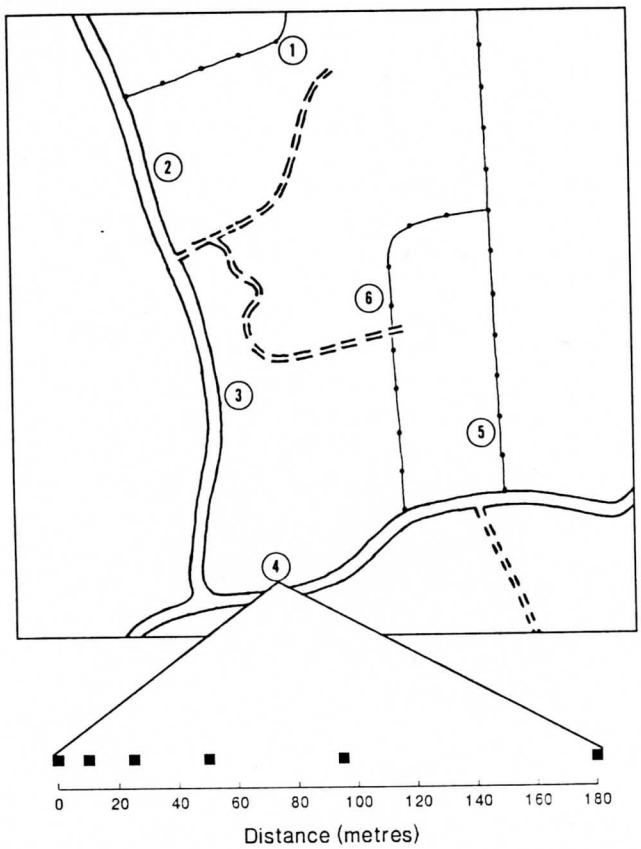

were established from capsules collected from three population categories within the census area: healthy (populations that had been healthy throughout the census period (1988–1993)), diseased (populations that had been diseased throughout), and newly established (populations which first appeared in the year in which seeds were collected). A total of eight families (by common female parent) of each type were established. Each family × history combination was represented once in each population.

Infected source plants were derived by inoculating healthy seedlings with one of six fungal lines obtained from spores collected from naturally diseased plants within the census area. Each of the six fungal lines was represented once in each array, with the order in the array being varied so as to produce a Latin square design (Sokal and Rohlf 1981).

Diseased and healthy plants grown up in the Duke University greenhouses were transported to MLBS in mid-May and transplanted into 20-cm pots. Arrays were set out in early June 1992 and censused throughout the growing season for new infection. For each individual, the number of flowers 21 days after flowering was initiated was recorded as a measure of flower production and each plant was examined

Fig. 2. Time to first appearance of new infections (given as number of days since the date of first flowering) in the experimental populations in relation to (*a*) population spacing and (*b*) population history (see text).

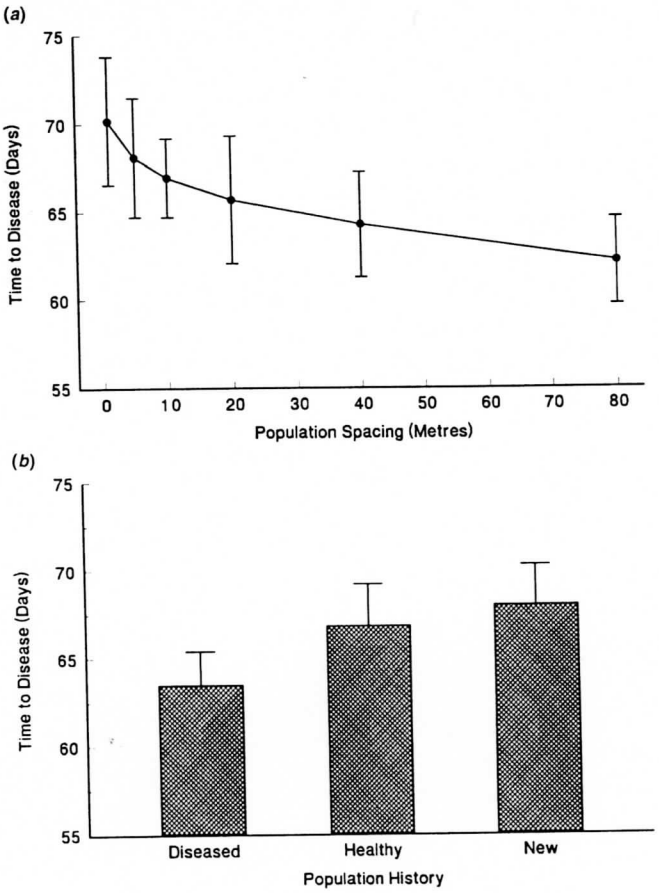

weekly for signs of new infection. During the course of the growing season, plants were fertilized at the beginning of June and July and watered weekly during dry periods.

Overall, 144 healthy plants became infected out of 864 target individuals. There were significant differences in disease spread among the replicates ($P = 0.010$), probably owing to differences in microenvironment; two of the replicates were located in less shady areas and consequently were more prone to drying out; there were almost no new infections in one of these (replicate 4, see Fig. 1).

The experiment was repeated in 1993, but only one newly diseased plant was observed, precluding any kind of inference regarding the effects of population spacing or history; the summer was unusually hot and dry and there were low infection rates in other associated field experiments at MLBS (S.M. Altizer, P.H. Thrall, and J. Antonovics, unpublished data). All the results discussed below are therefore for 1992 data.

Effects of population spacing on rates of spread

There was a nonsignificant ($P = 0.17$) trend for populations separated by larger distances to have a higher percent infection (analysis of variance on arcsin square root transformed data of percent disease per plot, weighted by the number of plants that became infected in each replicate). Disease appeared

significantly ($P = 0.02$) earlier in populations that were further apart (Fig. 2*a*; analysis of variance on time between first flowering and first appearance of disease, for those plants that became diseased).

Relationship between population history and resistance

There was a nonsignificant trend (analysis of variance, similar to above, $P = 0.16$) for higher levels of infection in plants that came from diseased populations (20%) than in plants that came from healthy populations (15%, healthy and newly established combined). There was a significant effect (analysis of variance similar to above, $P = 0.02$) of population history on time to infection (Fig. 2*b*): plants that became infected did so earlier when they came from diseased populations (mean time to first infection: 63 days) than when they came from healthy or newly established populations (67 days). However, there were no significant differences among the different history categories with respect to date of first flowering of plants that eventually became diseased, indicating that the difference in time to infection is not due to phenological differences.

Computer simulation: regional and temporal patterns

To understand better the dynamics of this natural host–pathogen system we developed a spatially explicit simulation model of sets of local populations incorporating both within-population dynamics and among-population dispersal, migration, and extinction processes. The model was parameterized using data from prior experiments (see Thrall and Jarosz 1994*a*, 1994*b*) and the field censuses (Antonovics et al. 1994*b*).

Within-patch dynamics

If X_t, Y_t, and N_t are respectively the numbers of healthy hosts, infected hosts, and total host population at time t, the rate at which individuals become diseased can be written as $\beta X_t Y_t / N_t$ if frequency-dependent disease transmission is assumed (Anderson 1981; Getz and Pickering 1983; Alexander and Antonovics 1988; Thrall et al. 1993*a*, 1994). β therefore represents a measure of the effectiveness of disease transmission.

A reasonable assumption, given the long time lag between the receipt of spores and the appearance of newly infected (and therefore sterile) flowers (Alexander 1990*b*), is that reproduction by healthy hosts occurs early during the growing season, and is followed by infection and (or) overwintering death. If the simplifying assumption of no host recovery is made, the basic model for host–pathogen dynamics with linear frequency-dependent disease transmission can be written as:

$$[1] \quad X_{1,t+1} = X_{1t}\left[b_1 + \left(1 - \beta_1 \frac{Y_t}{N_t}\right)(1 - d)\right]$$

$$[2] \quad X_{2,t+1} = X_{2t}\left[b_2 + \left(1 - \beta_2 \frac{Y_t}{N_t}\right)(1 - d)\right]$$

$$[3] \quad Y_{t+1} = Y_t\left(1 + \beta_1 \frac{X_{1t}}{N_t} + \beta_2 \frac{X_{2t}}{N_t}\right)(1 - d)$$

where d is the intrinsic death rate (data from both natural and experimental populations indicates that mean death rates for diseased hosts are not significantly different from healthy hosts); b_i is the birth rate, and β_i is the disease transmission parameter for the ith host type, respectively. In the simulation, we let X_1 represent the numbers of the more susceptible host and X_2 represent the numbers of the more resistant host ($\beta_1 > \beta_2$); a cost of resistance is included by assuming that $b_1 > b_2$. In this model, we assume a density-dependent per capita reproductive rate of the form

$$[4] \quad b_i = \frac{\lambda_i}{\gamma N_t + 1}$$

The parameter λ_i is the maximum reproductive rate of the ith host (i.e., the limit of N_t as it approaches zero) and γ is a constant that determines the strength of density dependence. The per capita reproductive rate (Eq. 4) declines hyperbolically as population density (N_t) increases. Such hyperbolic growth functions have been shown to be good representations of density-dependent growth in plant populations (Harper 1977; Thrall et al. 1989).

Earlier experimental studies using host lines that were either susceptible or resistant gave estimated values of β as 0.658 for susceptible hosts and 0.202 for resistant hosts (Thrall and Jarosz 1994*b*; see also Alexander 1990*a*, Alexander et al. 1993). The overall mean death rate for healthy and infected individuals combined, based on data from both natural and experimental populations, was assumed to be 0.5 (Thrall and Jarosz 1994*b*; H.M. Alexander and J. Antonovics, unpublished data). Values for birth rates (λ_i) of susceptible and resistant individuals were assumed to be 2.0 and 1.75, respectively (based on Thrall and Jarosz 1994*b*).

The census data indicated that sizes of populations that have always been present and healthy during the years of the study (1988–1994) were distributed according to a log-normal distribution. We made the assumption that the average size of these populations represented the distribution of carrying capacities. In the simulation, we therefore distribute the carrying capacities in the same proportions as observed in the natural metapopulation by varying the value of the parameter γ. Within each patch the dynamics are deterministic, but when numbers become less than one (i.e., fractional individuals), population sizes are set to zero.

Among-patch dynamics

After each time interval a small fraction, m, of the seeds and spores produced in a given patch at time t are dispersed according to a Weibull probability distribution, where the probability of landing in a site that is i units from the source site is given by

$$[5] \quad P(i) = e^{-\left(\frac{i}{\alpha}\right)^{\Theta}} - e^{-\left(\frac{i+1}{\alpha}\right)^{\Theta}}$$

and the parameters α and Θ control the scale and shape of the dispersal curve, respectively (Martz and Waller 1982). The fraction of seeds ($1 - m$) that remain within each patch are subject to density-dependent regulation (see Eq. 4 above); the fraction of seeds that migrate out of patches are not, although whether or not seeds that disperse out of patches actually colonize successfully is determined by a fixed probability of establishment.

Fig. 3. Host (*a*) and pathogen (*b*) extinction rates calculated as the fraction of populations present at time t that were absent at time $t + 1$. Populations were sorted into logarithmically increasing size classes (1, 2−3, 4−7, 8−15, 16−31, 32−63, 64−128, 128−255, >256) and an extinction rate was calculated for each class. The mean extinction rate for each size class (pooled over the years 1989−1993) was then regressed against the mean population size for each class using a hyperbolic function, $1/(1 + bN)$; the parameter b was detemined to be 1.133 for host populations (Fig. 5*a*) and 1.463 for pathogen populations (Fig. 5*b*).

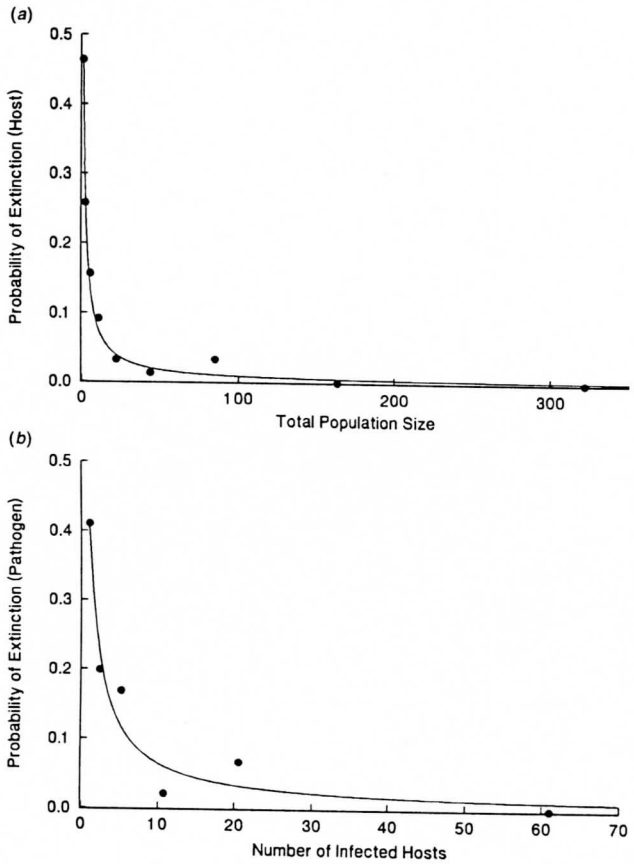

Results from earlier field studies have shown that both for the host and the pathogen, most dispersal is quite local (within 1−2 m for seeds and within 10 m for spores; Alexander 1990*b*; Antonovics et al. 1994*b*). For the simulation results reported here, we assume that both α and $\Theta = 1$ since these values result in dispersal curves approximating the empirical data (see Antonovics et al. 1994*b*). Following such migration (m was assumed to be 0.05), new numbers of hosts and pathogens are calculated for each patch and the dynamics and dispersal phase are repeated. In all cases, we considered both initial colonists and subsequent migrants as part of the within-population dynamics.

At each time interval, subsequent to the migration phase but prior to the within-population dynamics phase, a probability of extinction is calculated for each occupied patch. Estimates for both host and pathogen extinction rates were empirically determined from the census data (Fig. 3). Because an analysis of extinction rates in natural populations showed

Fig. 4. Relation between the size of diseased populations and percent infection. The plotted points are the means for the same size classes described in Fig. 3. The solid line represents data obtained from the computer simulation (means obtained from the last 10 generations of a single run using the default values; see text) and the dashed line represents data from the census of natural populations (means for the years 1988−1993).

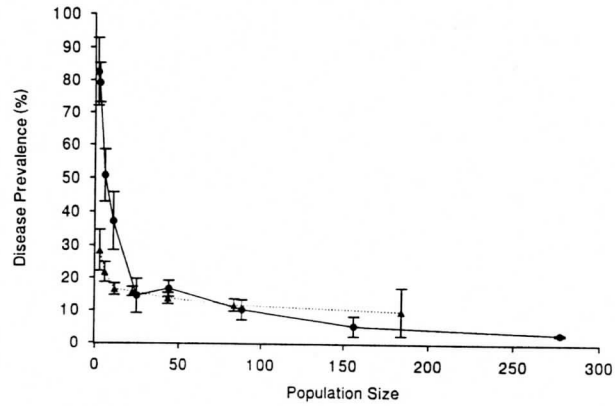

that there was a large effect of population size but a marginally nonsignificant effect of population status (healthy vs. diseased) in the model, extinction rates are assumed to be the same for healthy and diseased populations.

To start each simulation, 100 sites (out of 600 possible) are randomly filled with an equal number of susceptible and resistant individuals (initial frequency of resistance = 0.5). A subset of 20 of these initial populations is then randomly chosen to have the pathogen present at a frequency of 0.25. In the results reported here, each simulation was generally allowed to run for 300 generations, by which time spatial and temporal patterns (percent occupancy and disease levels) had generally become stable.

General fit to observed patterns from census data

A number of features of the computer simulations were in close qualitative agreement with the patterns observed in the natural metapopulation. For example, the census data over the last 7 years revealed a negative relationship between the size of diseased populations and percent infection (Fig. 4); a similar pattern was obtained from the simulation. In general, disease incidence and population size values from the census (Table 1) agreed qualitatively with results from the computer simulation where typical values were the following: mean population size, 43.6 (SE = ±0.8) for healthy populations and 67.7 (SE = ±2.2) for diseased populations; average percentage of populations with disease, 26.8 (SE = ±1.5); and mean percentage of infected individuals in diseased populations, 25.1 (SE = ±1.4). In both the simulation and field studies, the mean size of diseased populations was consistently larger than healthy ones. There was also a clear effect of disease on average population size and percent occupancy (on average, 20% occupancy with disease present and 40% with no disease after 300 generations). The visual impression from maps depicting the temporal and spatial results of a typical simulation run was consistent with the patchy distribution of disease observed in the natural metapopulation.

Fig. 5. Pearson product−moment correlation between resistance and disease frequency (calculated across all sites) from the simulation. Values shown are the means of five simulation runs, with data taken at five generation intervals within each run. Horizontal dashed line indicates a correlation of zero.

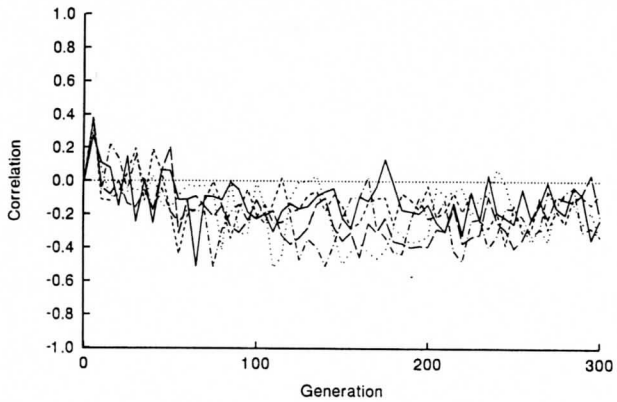

Fig. 6. Change in the mean frequency of resistance over time. Dashed lines represent five random runs of the simulation model with the disease absent but otherwise assuming the default parameter values (see text). The solid line is the predicted time to fixation for the susceptible type from the deterministic single population model (i.e., [1]−[3] with no spatial structure). Numbers on the right-hand side of the graph are the number of generations to fixation for each of the simulation runs.

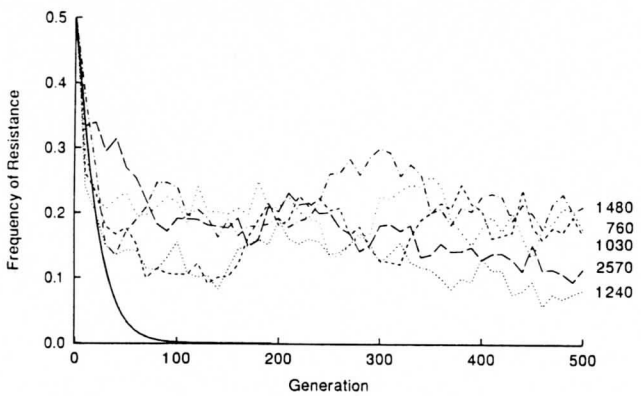

Population resistance structure

In all cases, there was an initial phase when local disease increase resulted in higher frequencies of the resistant type in those patches that were diseased. However, after a period of ca. 50 generations the relationship between disease level and resistance frequency became negative, suggesting that populations were less likely to become diseased if they were resistant (Fig. 5). At this point, many populations were fixed for either the susceptible or more frequently the resistant type (there were relatively few polymorphic populations), and visually, patches of high resistance generally had low (or occasionally intermediate) disease incidence; patches in which disease levels were high were always close to fixation for the susceptible type.

In general, whether positive or negative correlations between resistance and disease levels were found depended on rates of turnover, the history of the populations being sampled, and on the force of selection against the susceptible type when disease is present or against the resistant type (cost of resistance) when disease is absent. Generally, we would expect a negative correlation between resistance and disease prevalence if the disease is lost quickly as resistance spreads, if the cost of resistance is low, and if the disease is widespread and population turnover is high.

Fig. 7. Comparison of local (deterministic; dashed line) vs. regional (simulation; solid line) dynamics for two different sets of conditions: (*a*) predicted outcomes using field parameterized values (see text), (*b*) predicted outcomes assuming a high transmission rate for the susceptible host ($\beta_1 = 1.5$).

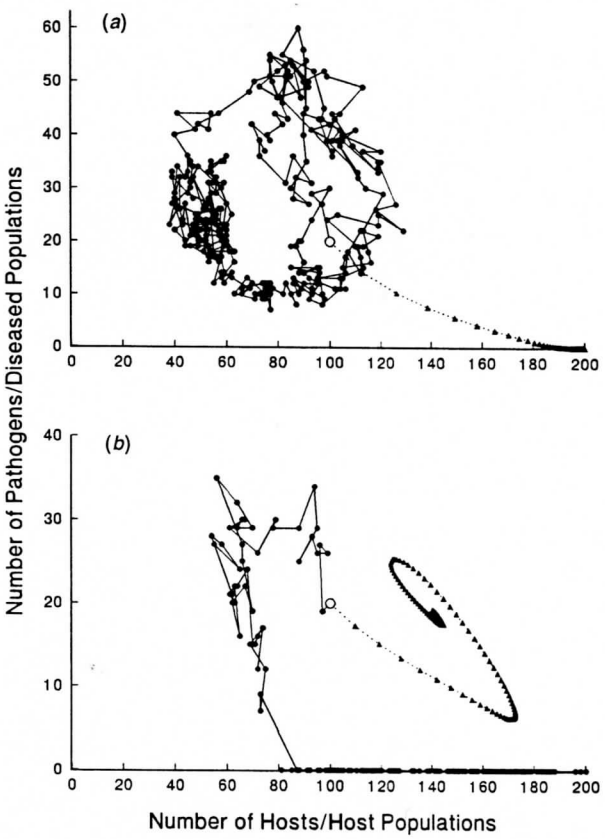

As expected, when the simulation was run without disease present but with the same initial number of populations and frequency of resistance, the resistant type was always lost from the metapopulation. However, the time to fixation for the susceptible host type was often in excess of 1000 generations (Fig. 6). For comparison, time to fixation was also calculated for a deterministic model without spatial structure using the same parameter values. In this case, the resistant type was lost in less than 100 generations, in general agreement with standard population genetic theory (Strickberger 1985).

Local vs. regional dynamics: connectedness and coexistence

When the empirically estimated values for disease transmission rates, host birth rates, and death rates were used, in 25 out of 100 runs, the simulation model resulted in coexistence

of both host types with the pathogen; in the other cases, the pathogen was lost with eventual fixation of the susceptible type. This loss, if it occurred, was usually rapid and occurred within the first 50 generations, suggesting that stochastic factors were important in establishment and initial spread of the pathogen. When Eqs. 1–3 were iterated for a single population using the default parameter values (and with the disease initially present), the predicted outcome was extinction of the pathogen and eventual fixation of the susceptible host type (Fig. 7*a*). Alternatively, when a somewhat higher disease transmission rate was assumed for the susceptible host ($\beta_1 = 1.5$), the within population model predicted coexistence of both host types with the pathogen, while the simulation model invariably (out of 100 runs) resulted in rapid loss of the pathogen and fixation of the susceptible type (Fig. 7*b*).

Discussion

Traditionally, population biologists have studied coexistence and genetic polymorphism in single closed populations, and theories based on such populations have served as useful null models (e.g., the Hardy–Weinberg model for population genetics). However, the increased complexity possible in spatially structured systems makes it difficult to envision how such single population models should be applied to the systems of interacting populations that are likely to be commonplace in nature (Hanski and Gilpin 1991; Frank 1992, 1993).

Our results from the simulation studies indicate that incorporating spatial structure into models of host–pathogen systems can have dramatic effects on conditions for host and pathogen coexistence. For example, we have shown that coexistence can be enhanced in spatially structured sets of populations because exportation of spores effectively increases the transmission rate and the pathogen can be rescued from extinction. However, metapopulation structure does not invariably increase coexistence because some values that resulted in polymorphism and coexistence with the pathogen for a single population caused extinction in the spatial simulation. The difference between metapopulation and single population approaches was most forcefully illustrated in the simulation runs for situations when no disease was present, and where there was a cost to the resistance such that the resistance allele was disadvantageous. It generally took a very long time (often in excess of 1000 generations) for the resistant type to be completely lost from the metapopulation system, which was in stark contrast to the results for loss of disadvantageous alleles in single populations (as is usually considered in classical population genetics theory). It seems likely that loss of resistant types is slower in spatially structured systems because colonies are often founded only by one genotype. If new colonies are composed mostly of either the susceptible or resistant type alone, then selection operates primarily at the level of populations rather than among individuals; the life span of populations is far longer than that of individuals, and therefore, the selection process is much slower. Given the high rates of colonization and extinction that occur in the *Silene* populations, selection is transformed from a predominantly among-individual process into a predominantly group-level process. This hypothesis was supported by the fact that when simulations were run in which the degree of dispersal was much greater, the time to extinction for the resistant type (in the absence of disease) was much less; similarly when populations were constrained to behave as independent units with no dispersal at all, the resistant type was lost in approximately the same number of generations as predicted by theory based on single populations.

Our studies have shown that with appropriate sampling procedures and choice of system, it is possible to study multiple populations simultaneously and over extended time spans. In our censuses we do not attempt to obtain accurate demographic information on individuals but count only flowering plants (although we do record nonflowering individuals when they are seen), and our census occurs once a year, so we ignore within-season changes (although we do check critical extinctions of the host or pathogen in a second recensus later in the season). Nevertheless, it is still possible to obtain a detailed and informative picture of metapopulation structure in the form of estimates of colonization and extinction rates for hosts and pathogens, average population size for healthy and diseased populations, population growth rates, and patterns of disease incidence. However, such straightforward census data do not provide ready clues to the causal factors that have produced the observed patterns, especially given the complexity of the within-population dynamics, the various factors (intrinsic and extrinsic) that can affect extinction, and the superimposed migration and colonization processes. The computer simulation studies are therefore a necessary adjunct to understanding the processes that give rise to the patterns observed in natural populations. Such studies provide a means by which we can do computer experiments that would not be possible in the real world. For example, we can show that the negative relationship between disease incidence and population resistance is likely to be a general feature of long established systems, where resistance costs are low and population turnover is high.

Moreover, by systematically varying parameters for which estimates are difficult to obtain (e.g., actual spore migration rates among patches), it is possible to ask whether variation in these parameters would influence outcomes that can be observed in the natural populations, and therefore, whether their measurement and estimation should be a critical component of a research program. It is very obvious to us that the simulation model presented here is a reflection of the current state of knowledge about the *Silene–Ustilago* system and as such is only a rough approximation of nature, which perforce ignores many details of the biology. For example, we still have no clear understanding of many details of pollinator dynamics or behavior even though there is evidence that pollinators discriminate between healthy and diseased flowers (Roche 1993; B.M. Roche, H.M. Alexander, and A. Maltby, unpublished data; S.M. Altizer, P.H. Thrall, and J. Antonovics, unpublished data). Such behavior could have a significant impact on dynamics, especially if the degree of discrimination was itself frequency dependent (Real et al. 1992).

The very process of constructing a simulation model can also pinpoint aspects of a system that are poorly understood biologically but which may have a substantial impact on the outcome; for example, while there is considerable evidence that disease transmission within populations is frequency dependent, the model currently assumes that export of spores from populations is not a function of frequency but of absolute density of diseased individuals. We have no idea whether this is true because prior to the simulation it had not occurred to us to ask whether the processes of intrapopulation trans-

mission were different from the processes of interpopulation transmission. Immediately, it becomes evident that there is a need for further experiments.

Experimental arrays of populations allow us to test general ideas about the effect of different degrees of connectedness on establishment and persistence and to test some a priori notions about resistance structure (e.g., our idea that resistance levels might be higher in populations with a history of disease than ones without such a history). Agreement between experimental results and those from computer simulation studies can therefore provide much confidence in interpreting the observed patterns. For example, we had initially predicted a positive correlation between resistance and disease levels; the finding of a negative relationship in the experimental metapopulations arrays caused us some dismay until the simulation study produced the same result independently! The fact that disease spread was greater in more isolated populations suggests that pollinators may be limited in this system (cf. Alexander 1987; Antonovics and Alexander 1993) with isolated populations attracting a disproportionate share of visits on a per individual plant basis; similar effects have been frequently reported for more isolated individuals in plant–herbivore systems (Antonovics and Levin 1980). This result was in fact the opposite of what we had expected, pointing to the need for more detailed studies of vector dynamics and behavior.

The main lesson from our studies is that understanding and predicting host and pathogen abundances, and resistance and virulence structure are likely to be impossible without detailed longitudinal studies of multiple populations. In addition, because of the complexity of the interactions, detailed studies of a wide range of populations have to be critically integrated with experimental and simulation studies so as to obtain an understanding of the processes involved in the regional as well as local dynamics of host–pathogen systems. Dynamics in a single population may represent the outcome of serendipitous local conditions, may be influenced by unmeasured processes of immigration and emigration, and may be in part determined by genotypic composition determined by stochastic events during the founding of the population. The intense and specific study of one or a few populations may be very misleading.

Acknowledgements

The support of National Science Foundation Grant DEB-9119626 is gratefully acknowledged. We would also like to acknowledge Mark Givens for permission to use his land, and the assistance of S.M. Altizer, E.J. Lyons, C. Nelson, T. Preuninger, and S.J. Burckhalter with setting up and maintaining the experimental metapopulation experiment over the last 3 years. Without their willingness to battle the quirks of electric fences, stampeding cattle, poison-ivy, and marauding grasshoppers, the experimental work would not have been possible. This paper was improved by the comments and suggestions of A.D. Rayner.

References

Alexander, H.M. 1987. Pollination limitation in a population of *Silene alba* infected by the anther smut fungus, *Ustilago violacea*. J. Ecol. **75**: 771–780.

Alexander, H.M. 1990*a*. An experimental field study of anther-smut disease of *Silene alba* caused by *Ustilago violacea*: genotypic variation and disease incidence. Evolution, **43**: 835–847.

Alexander, H.M. 1990*b*. Epidemiology of anther-smut infection of *Silene alba* caused by *Ustilago violacea*: patterns of spore deposition and disease incidence. J. Ecol. **78**: 166–179.

Alexander, H.M., and Antonovics, J. 1988. Disease spread and population dynamics of anther-smut infection of *Silene alba* caused by the fungus *Ustilago violacea*. J. Ecol. **75**: 91–104.

Alexander, H.M., and Maltby, A. 1991. Anther-smut infection of *Silene alba* caused by *Ustilago violacea*: factors determining fungal reproduction. Oecologia, **84**: 249–253.

Alexander, H.M., Antonovics, J., and Kelly, A. 1993. Genotypic variation in plant disease resistance: physiological resistance in relation to field disease transmission. J. Ecol. **81**: 325–334.

Anderson, R.M. 1981. Population dynamics of indirectly transmitted disease agents: the vector component. *In* Vectors of disease agents. *Edited by* J.J. McKelvey, Jr., B.F. Eldridge, and K. Maramorosch. Praeger, New York. pp. 13–43.

Anderson, R.M., and May, R.M. 1981. The population dynamics of microparasites and their invertebrate hosts. Philos. Trans. R. Soc. London B Biol. Sci. **291**: 451–524.

Antonovics, J. 1992. Toward community genetics. *In* Plant resistance to herbivores and pathogens. *Edited by* R.S. Fritz and E.L. Simms. University of Chicago Press, Chicago, Ill. pp. 426–449.

Antonovics, J. 1994. The interplay of numerical and gene-frequency dynamics in host–pathogen systems. *In* Ecological genetics. *Edited by* L. Real. Princeton University Press, Princeton, N.J. pp. 129–145.

Antonovics, J., and Alexander, H.M. 1993. Epidemiology of anther-smut infection of *Silene alba* (= *S. latifolia*) caused by *Ustilago violacea*: patterns of spore deposition in experimental populations. Proc. R. Soc. London B Biol. Sci. **250**: 157–163.

Antonovics, J., and Levin, D.A. 1980. The ecological and genetic consequences of density-dependent regulation in plants. Annu. Rev. Ecol. Syst. **11**: 411–452.

Antonovics, J., and Thrall, P.H. 1994. The cost of resistance and the maintenance of genetic polymorphism in host–pathogen systems. Proc. R. Soc. London B Biol. Sci. **257**: 105–110.

Antonovics, J., Iwasa, Y., and Hassell, M.P. 1994*a*. A generalized model of parasitoid, venereal, and vector-based transmission processes. Am. Nat. In press.

Antonovics, J., Thrall, P.H., Jarosz, A.M., and Stratton, D. 1994*b*. Ecological genetics of metapopulations: the *Silene–Ustilago* plant–pathogen system. *In* Ecological genetics. *Edited by* L. Real. Princeton University Press, Princeton, N.J. pp. 146–170.

Baker, H.G. 1947. Infection of species of *Melandrium* by *Ustilago violacea* (Pers.) Fuckel and the transmission of the resultant disease. Ann. Bot. (London), **11**: 333–348.

Batcho, M., and Audran, J. 1980. Données cytochimiques sur les anthères de *Silene dioica* parasitées par *Ustilago violacea*. Phytopathol. Z. **99**: 9–25.

Boerlijst, M.C., Lamers, M.E., and Hogeweg, P. 1993. Evolutionary consequences of spiral waves in a host–parasitoid system. Proc. R. Soc. London B Biol. Sci. **253**: 15–18.

Brefeld, O. 1921. Investigations in the general field of mycology (Part XIII). Heinrich Schöningh, Münster.

Caswell, H. 1978. Predator-mediated coexistence: a non-equilibrium model. Am. Nat. **112**: 127–154.

Clinton, G.P. 1904. North American Ustilagineae. Proc. Boston Soc. Nat. Hist. **31**: 329–529.

Comins, H.N., Hassell, M.P., and May, R.M. 1992. The

spatial dynamics of host–parasitoid systems. J. Anim. Ecol. **61**: 735–748.

Farlow, W.G., and Seymour, A.B. 1888. A provisional host-index of the fungi of the United States. Cambridge University Press, Cambridge, England.

Farr, D.F., Bills, G.F., Chamuris, G.P., and Rossman, A.Y. 1989. Fungi on plants and plant products in the United States. The American Phytopathological Society, St. Paul, Minn.

Felman, Y.M. 1986. Sexually transmitted diseases. Churchill Livingstone, New York.

Frank, S.A. 1992. Models of plant–pathogen coevolution. Trends Genet. **8**: 213–219.

Frank, S.A. 1993. Coevolutionary genetics of plants and pathogens. Evol. Ecol. **7**: 45–75.

Getz, W.M., and Pickering, J. 1983. Epidemic models: thresholds and population regulation. Am Nat. **121**: 892–898.

Gilpin, M.E. 1975. Group selection in predator–prey communities. Princeton University Press, Princeton, N.J.

Hanski, I., and Gilpin, M. 1991. Metapopulation dynamics: brief history and conceptual domain. Biol. J. Linn. Soc. **42**: 3–16.

Harper, J.L. 1977. Population biology of plants. Academic Press, London.

Hassan, A., and MacDonald, J.A. 1971. *Ustilago violacea* on *Silene dioica*. Trans. Br. Mycol. Soc. **56**: 451–461.

Hassell, M.P., Comins, H.N., and May, R.M. 1991. Spatial structure and chaos in insect population dynamics. Nature (London), **353**: 255–258.

Holmes, K.K. 1983. International perspectives on neglected sexually transmitted diseases: impact on venereology, infertility, and maternal and infant health. McGraw-Hill, New York.

Jennersten, O. 1983. Butterfly visitors as vectors of *Ustilago violacea* spores between caryophyllaceous plants. Oikos, **40**: 125–130.

Jennersten, O. 1988. Insect dispersal of fungal disease: effects of *Ustilago* infection on pollinator attraction in *Viscaria vulgaris*. Oikos, **51**: 163–170.

Lee, J.A. 1981. Variation in the infection of *Silene dioica* (L.) Clairv. by *Ustilago violacea* (Pers.) Fuckel in North West England. New Phytol. **87**: 81–89.

Levin, S.A., and Udovic, J.D. 1977. A mathematical model of coevolving populations. Am. Nat. **111**: 657–675.

Levins, R. 1969. Some demographic and genetic consequences of environmental heterogeneity for biological control. Bull. Entomol. Soc. Am. **15**: 237–240.

Martz, H.F., and Waller, R.A. 1982. *Bayesian Reliability Analysis*. John Wiley & Sons, New York.

May, R.M., and Anderson, R.M. 1990. Parasite–host coevolution. Parasitology, **100**: S89–S101.

McNeill, J. 1977. The biology of Canadian weeds. 25. *Silene alba* (Miller) E.H.L. Krause. Can. J. Plant Sci. **57**: 1103–1114.

Real, L.A., Marschall, E.A., and Roche, B.M. 1992. Individual behavior and pollination ecology: implications for the spread of sexually transmitted plant diseases. *In* Individual based models and approaches in ecology: populations, communities, and ecosystems. *Edited by* D.L. DeAngelis and L.J. Gross. Chapman and Hall, New York. pp. 492–508.

Roche, B.M. 1993. The role of behavior in a pollinator-mediated plant–pathogen interaction. Ph.D. Thesis, University of North Carolina, Chapel Hill, N.C.

Seymour, A.B. 1929. Host-index of the fungi of North America. Harvard University Press, Boston, Mass.

Sokal, R.R., and Rohlf, F.J. 1981. Biometry. W.H. Freeman and Company, New York.

Strickberger, M.W. 1985. Genetics. Macmillan Publishing Company, New York.

Thrall, P.H., and Jarosz, A.M. 1994*a*. Host–pathogen dynamics in experimental populations of *Silene alba* and *Ustilago violacea*. I. Ecological and genetic determinants of disease spread. J. Ecol. **82**: 549–559.

Thrall, P.H., and Jarosz, A.M. 1994*b*. Host–pathogen dynamics in experimental populations of *Silene alba* and *Ustilago violacea*. II. Experimental tests of theoretical models. J. Ecol. **82**: 561–570.

Thrall, P.H., Pacala, S.W., and Silander, J.A., Jr. 1989. Oscillatory dynamics in populations of an annual weed species *Abutilon theophrasti*. J. Ecol. **77**: 1135–1149.

Thrall, P.H., Antonovics, J., and Hall, D.W. 1993*a*. Host and pathogen coexistence in vector-borne and venereal diseases characterized by frequency-dependent disease transmission. Am. Nat. **142**: 543–552.

Thrall, P.H., Biere, A., and Antonovics, J. 1993*b*. Plant life history and disease susceptibility: the occurrence of *Ustilago violacea* on different species within the Caryophyllaceae. J. Ecol. **81**: 489–498.

Thrall, P.H., Biere, A., and Uyenoyama, M.K. 1994. Frequency-dependent disease transmission and the dynamics of the *Silene–Ustilago* host–pathogen system. Am. Nat. In press.